Skin Research & Technology

Micro-Relief Analysis with Skin Capacitive Imaging

SCHOLARONE™
Manuscripts

Micro-Relief Analysis with Skin Capacitive Imaging

Christos Bontozoglou[1,2], Xu Zhang[1*] and Perry Xiao[1,2]

[1] School of Engineering, London South Bank University, 103 Borough Road, London SE1 0AA, UK

[2] Biox Systems Ltd, Technopark Building, 90 London Road, London SE1 6LN, UK

Corresponding author: Christos Bontozoglou (MSc)
School of Engineering, London South Bank University, 103 Borough Road, London SE1 0AA, UK
Biox Systems Ltd, Technopark Building, 90 London Road, London SE1 6LN, UK
Postal address: 318 St John Street, London, EC1V 4NT, UK
E-main: bontozoc@lsbu.ac.uk

Co-author 1: Dr. Xu Zhang (PhD)
School of Engineering, London South Bank University, 103 Borough Road, London SE1 0AA, UK
*Current institution: Auckland Tongji Medical & Rehabilitation Equipment Research Centre, Tongji Zhejiang College, No 168 Business Road, Zhejiang, China, 314051

Co-author 2: Dr. Perry Xiao (PhD)
School of Engineering, London South Bank University, 103 Borough Road, London SE1 0AA, UK
Biox Systems Ltd, Technopark Building, 90 London Road, London SE1 6LN, UK

Keywords: skin micro-relief, image processing, hydration mapping, skin aging.

Running title: Skin Microrelief Analysis with Capacitive Imaging

Abstract

Background: In this study, the performance of capacitive imagining in skin micro-relief analysis was investigated. This measurement principle has been used for skin hydration measurements over the last decade and it is commercially available by various manufacturers. Strengthening its potential for new applications could offer an affordable and portable multi-purpose device for in-vivo skin research. Previous studies in the literature [1-10] have used a wide range of optical devices to determine how the skin surface topographic features are affected by chronological age, environmental influences and living habits.

Material and Methods: A capacitive system was used in order to capture hydration images from the middle volar forearm of twelve volunteers. The visual output of the system was studied and image processing algorithms were adapted to automatically extract skin micro-relief features. The change in the skin network of lines during arm extension, the lines' anisotropy index and the number of closed polygons per skin surface area were plotted against subjects' chronological age. The results were compared with optical measurements from the literature to validate our algorithms and evaluate the capacitive imaging in skin micro-relief analysis.

Results: The change in the intensity of primary and secondary lines during arm extension and the number of closed polygons per surface area were in agreement with the literature. The anisotropy index output gave inconclusive results.

Conclusions: The experimental results show that the capacitive systems could only extract two-dimensional skin topographic features.

Introduction

The skin is the largest organ of mammals in terms of surface and weight, as well as the one that is most exposed to the environment [1]. It is divided in multiple layers with stratum corneum being the outermost layer and source of information for many non-invasive instruments. The surface of stratum corneum has micro-structures that change with chronological age, environmental influences and living habits e.g. UV light exposure, alcohol and smoking etc [2]. These structures consist of a network of lines which can also be described as a collection of closed polygons [3]. Scientists in the field of skin research have used a variety of measurement principles to study either the network of lines or the closed polygons between them and found correlations with living habits and age.

Corcuff et al. [4] used images of rotating negative volar forearm replicas under oblique illumination to study the network of lines and its response during arm extension in different age groups. They found that the skin micro-relief has main lines in either one or two orientations and that the percentage of people in the second category decreases with age. Moreover, they measured that young people buffer strain between these groups of lines during arm extension, while elderly tend to have one orientation which rotates. The lines in one orientation relate to Langer's line, have depth greater then 60μm and increase in intensity with age [5]. The lines in the second orientation relate to the tension effect of elastic fibres network, are sallower and fade with age [5].

Zahouani et al. [5] used a scalar value, the anisotropy index, to represent the above observations and successfully correlated it with chronological age based on 3D confocal microscopy images from volar forearm of 120 Caucasian women. The anisotropy index of skin micro-relief is defined as: "the

level of anisotropy, i.e. the percentage of furrows oriented in a different direction. It is the ratio of the minimal spectral moment of the surface to the maximal spectral moment of the surface. The higher this level, the greater the anisotropy of the surface, i.e. the less the furrows are uniformly oriented in all directions" [6]. Since one orientation of skin lines intensifies and the second fades with age, the Anisotropy Index is proportional to skin ageing.

Gao et al. [7] used an image acquisition device alongside a segmentation algorithm to count the number of closed polygons (NCP) automatically and they verified its reliability by comparing results with manual counting in dorsal hand of 100 subjects. They found that the NCP correlates negatively and the standard deviation of polygons' area correlates positively with age, lifetime of sun-exposure and Beagley-Gibson score. This means that younger people tend to have smaller and more uniform polygons in dorsal hand. Their findings are in agreement with [3], where Trojahn et al. studied the NCP and skin roughness against chronological age in volar forearm using a UVA-light camera. The latter group concluded that the NCP correlates with age but not with skin toughness.

Most of these studies depend on light-based devices and 3D skin replicas to allow micro-topographic feature extraction. Recently, capacitive imaging systems for skin hydration measurements are becoming commercially available. These are more affordable and portable than conventional skin imaging systems and studies indicate they can provide equivalent information on skin topographic analysis. Lévêque and Querleux [8] achieved to detect the micro-relief orientation, calculate the number of intersections and the corners' density. Bevilacqua et al. [1] detected the main relief orientations but also produced a wrinkles-enhanced image and developed algorithm to count the skin closed polygons automatically [9]. The latter group stretched technology further by equipping the device with a pressure sensor and achieving accurate wrinkles' depth profiling up to 50μm [10].

In the following sections, the imaging system Epsilon E100 is presented alongside existing algorithms for skin micro-relief feature extraction and suggested alterations for application on capacitive images. Then, experimental results achieved with a small group of volunteers are compared with the literature in order to evaluate the performance of capacitive imaging in micro-relief analysis.

Materials and Methods

Epsilon E100 capacitive imaging system

Our study is based on Epsilon E100 (Biox Systems Ltd., London UK) to capture skin hydration images and the results are produced with the analysis suites of the provided software. The overall sensing area of the probe is 12.8x15mm and it is filled with an array of 256x300 pixels (50μm resolution). Its major advantage, over other capacitive skin hydration systems, is the calibrated response to near-surface dielectric permittivity (ε). This ensures that the sensor doesn't saturate when samples have low hydration and it maintains constant sensitivity across the whole scale [11]. In the software, the visual representation of ε is black for the lowest dielectric permittivity and becomes brighter with permittivity increment [12].

Except for capturing snapshots, the software allows to analyse them using a circular region of interest and a permittivity filter (ε-filter). These play important role in our study because they focus the results on different skin components. Figure 1 illustrates how unwanted components can be excluded (greyed-out) from a capacitive image of volar forearm. In the first snapshot, the unprocessed image, the areas of skin in contact with the sensor appear in green colour while the

areas not in contact with the sensor (i.e. skin lines, furrows and borders) appear dark. Also, one may notice a few bright spots that indicate sweat gland activity. The middle snapshot demonstrates how ε-filter removes borders' bad contact, skin lines and sweat spots to focus the analysis output on the skin. After the ε-filter application the mean dielectric permittivity increases and the standard deviation decreases, since both become representative of the skin and not of a mean between skin, sweat and bad contact. The last image shows how the skin and sweat information can be excluded with the ε-filter and the borders with a circular region of interest. This maintains only the information on skin lines and furrows, which can be useful in skin micro-relief analysis.

Skin Micro-Relief Orientation

To the best of our knowledge, Lévêque and Querleux first suggested the use of contact imaging systems to study skin micro-relief alongside hydration. In their study [8], they converted their 256-gray-level image to a 5-gray-level image, they calculated the Grey-Level Co-occurrence Matrix (GLCM) and they plotted the correlation feature against different angles allowing the detection of skin primary lines orientations. The co-occurrence matrix P, of a dielectric permittivity image I, for displacement d and angle θ is presented by [13]:

$$P(i,j,d,\theta) = \sum_{x=0}^{n} \sum_{y=0}^{m} \delta_{iI_1}\delta_{jI_2} \quad (1)$$

where, δ_{kl} Kronecker delta,
$I_1 = I(x,y)$ and
$I_2 = I(x + d\cos\theta, y + d\sin\theta)$

Then, the correlation feature can be extracted by:

$$COR(d,\theta) = \frac{\sum_{i=0}^{G-1} \sum_{j=0}^{G-1} ij\hat{P}(i,j,d,\theta) - \mu_1\mu_2}{\sigma_1^2 \sigma_2^2} \quad (2)$$

where, G the ε-tone levels and
μ and σ the mean and standard deviation correspondingly.

The GLCM correlation values can be then represented in a polar graph, as in Figure 2.

Targeting Feature Orientation with ε-filtering

According to the developers of GLCM [14], the correlation feature "is a measure of grey-tone linear-dependencies in the image", so the output of this algorithm is affected by all structures of the skin surface. It indicates the average direction of all components in the image, not only the skin lines, and results to distorted anisotropy index. In order to overcome this problem, the capacitive image can be quantised into three non-uniform levels using the ε-filter. As a result, the algorithm focuses on features in specific permittivity value range, it executes faster and has lower output noise. The drawback of this approach is that textural information is lost and image classification capabilities are faded [15], but these aspects are not related to our present study. The effect on the angular distribution as well as on the anisotropy index can be seen in Figure 2, where the same image is studied with and without ε-filter.

Skin Closed Polygons

Researchers in [7] achieved successful automatic counting of skin closed polygons using a morphological image processing approach. Unfortunately, capacitive images have five times less resolution than their light-based images and similar approaches are not applicable. Any morphological window will either be very wide, hiding micro-relief components, or small enough to be ineffective. The solution to this problem is given by [9] with the use of a gradient-based segmentation, the Vincent and Soille [16] watershed segmentation. In layman terms, the algorithm performs a gradient descent from local maxima to produce watersheds, i.e. crossing lines that separate the skin closed polygons, while counting the surface area of each closed polygon [17]. A visual example of this algorithm output is illustrated in Figure 3.

Experiment & Results

In order to validate these algorithms and evaluate the use of capacitive imaging systems for skin micro-relief analysis an experiment with 12 volunteers was conducted and the results were compared with the literature. For this purpose, two capacitive images are captured from the middle volar forearm of each volunteer, one with elbow at 90° and one at 180°. In both cases the arm was relaxed and the palm was open towards the body core. These images were fed to the suggested algorithms and the results were plotted against the subjects' chronological age. The parameters of interest are: (a) the sum of absolute correlation change of primary and secondary lines during arm extension (Figure 4), (b) the anisotropy index (Figure 5) and (c) the number of closed polygons per surface area (Figure 6). At this point we need to mention that samples from the two younger subjects with arm in extension are missing from our dataset, so they were excluded from the first experiment.

The first parameter derives from the GLCM correlation feature output (eq. 1 and 2). The correlation magnitude of primary and secondary lines was recorded manually and their absolute change when the elbow angle changes from 90° to 180° was calculated. According to the literature, young people buffer the strain between primary and secondary lines, expecting their intensity to remain more stable than in elderly subjects during arm extension. The anisotropy index results calculated according to [5] using again the GLCM correlation feature percentage (eq. 1 and 2). For this analysis the images recorded with elbow at 90° were used in order to ensure the arm is in resting position. For the last parameter of interest, the capacitive images recorded at resting position were used alongside the Vincent and Soille segmentation algorithm to automatically calculate the number of skin closed polygons per surface area. The negative correlation of 0.7 comes in agreement with the literature, demonstrating how skin closed polygons increase in size with chronological age.

Conclusions

In this study, we have achieved to develop an image processing tool for capacitive imaging systems with purpose to evaluate the capability of such devices in skin micro-relief analysis. The tool is based on two algorithms widely used in this field, the Grey-Level Co-occurrence Matrix and the Vincent and Soille segmentation. In order to evaluate their performance, an experiment was conducted, the results were plotted against the subjects' chronological age and their consistency with the literature is examined.

We conclude that the capacitive imaging sensors are capable of skin micro-relief analysis when the latter does not depend on depth measurements. More specifically, they are able to detect the orientation of skin primary and secondary lines as well as the size of individual closed polygons, since the experimental results achieved in these cases come in agreement with the literature. The change of intensity in primary and secondary lines during arm extension (Figure 4) and the number of skin closed polygons per surface area (Figure 6) show conclusive results on subject age classification. Unfortunately, the system is unable to calculate the anisotropy index correctly, although the analysis is based on the same dataset and image processing algorithms. Major source of error is the inability of such sensory system to measure the depth of skin lines, which results to inclusion of tertiary and quaternary lines in the calculation of anisotropy index. Secondary source could be the skin surface deformation during measurements due to the measurement principle itself.

Future Work

The present work gives solid answers to our primary research questions, but it also generates many new ones. The two dimensional analysis seems successful, but the absolute readouts cannot be confirmed until they are converted to SI distance units, directly comparable with calibrated digital spectroscopy. An important error is expected because all the above algorithms are affected both by the length and width of skin lines. Detecting and subtracting this error will increase the reliability, but also calculating the width of skin lines can itself extend the applications of capacitive imaging in skin surface analysis.

To the best of our knowledge, segmentation algorithms have been used extensively in skin micro-relief analysis, but information about individual skin closed-polygon has not been utilised. Applying pattern recognition algorithms could allow locating a specific enclosed polygon in multiple capacitive skin images and tracking any changes in size and shape over time. Except for skin closed-polygons, this could be also applied in other skin surface artefact, such as moles and scares etc.

Acknowledgments

References

[1] A. Bevilacqua, A. Gherardi, and R. Guerrieri, "In Vivo Quantitative Evaluation of Skin Ageing by Capacitance Image Analysis," in *Application of Computer Vision, 2005. WACV/MOTIONS '05 Volume 1. Seventh IEEE Workshops*, Breckenridge, CO, 2005, pp. 342-347.

[2] B. Isik, M. S. Gurel, A. T. Erdemir, and O. and Kesmezacar, "Development of skin aging scale by using dermoscopy," *Skin Res Technol*, vol. 19, no. 2, pp. 69-74, 2013.

[3] C. Trojahn et al., "Relation between skin micro-topography, roughness, and skin age," *Skin Res Technol*, vol. 21, no. 1, pp. 69-75, 2015.

[4] P Corcuff, O de Lacharrière, and JL. Lévêque, "Extension-induced changes in the microrelief of the human volar forearm: variations with age," *Journal of gerontology*, vol. 46, no. 6, pp. M223-

7, 1991.

[5] H Zahouani, M Djaghloul, R Vargiolu, S Mezghani, and M.E.L Mansori, "Contribution of human skin topography to the characterization of dynamic skin tension during senescence: morpho-mechanical approach," *Journal of Physics: Conference Series*, vol. 483, p. 012012, 2014.

[6] J.M. Lagarde, C. Rouvrais, and D. Black, "Topography and anisotropy of the skin surface with ageing," *Skin Research and Technology*, vol. 11, no. 2, pp. 110–119, 2005.

[7] Q. Gao et al., "Automatic measurement of skin textures of the dorsal hand in evaluating skin aging," *Skin Res Technol*, vol. 19, no. 2, pp. 145-151, 2013.

[8] J. L. Lévêque and B Querleux, "SkinChip®, a new tool for investigating the skin surface in vivo," *Skin Research and Technology*, vol. 9, no. 4, pp. 343-347, 2003.

[9] A. Bevilacqua and A. Gherardi, "Age-related skin analysis by capacitance images," in *Proceedings of the 17th International Conference on Pattern Recognition*, vol. 2, 2004, pp. 703-706.

[10] A. Bevilacqua and A. Gherardi, "Characterization of a capacitive imaging system for skin surface analysis," in *First Workshops on Image Processing Theory, Tools and Applications*, 2008, pp. 1-7.

[11] W. Pan, X. Zhang, E. Chirikhina, C. Bontozoglou, and P. Xiao, "Measurement of Skin Hydration with a Permittivity Contact Imaging System," in *23. IFSCC Conference*, Zurich, 2015. [Online]. http://tst.pg2.at/abstracts/a0015.html?zoom_highlight=

[12] P. Xiao and C. Bontozoglou, "Capacitive contact imaging for in-vivo hair and nail water content measurements," *H&PC Today*, vol. 10(5), pp. pp62-65, September/October 2015.

[13] F. Bianconi, E. Chirikhina, F. Smeraldi, C. Bontozoglou, and P. Xiao, "Personal identification based on skin texture features from the forearm and multi-modal imaging," *Skin Res Technol*, vol. 23, no. 3, pp. 392-398, 2017.

[14] R. M. Haralick, K. Shanmugam, and I. Dinstein, "Textural Features for Image Classification," in *IEEE Transactions on Systems, Man, and Cybernetics*, vol. SMC-3, 1973, pp. 610-621.

[15] D. A. Clausi, "An analysis of co-occurrence texture statistics as a function of grey level quantization," *Canadian Journal of Remote Sensing*, vol. 28, pp. 45-62, 2002.

[16] L. Vincent and P. Soille, "Watersheds in digital spaces: an efficient algorithm based on immersion simulations," in *IEEE Transactions on Pattern Analysis and Machine Intelligence*, vol. 13, Jun 1991, pp. 583-598.

[17] R. Achanta et al., "SLIC Superpixels Compared to State-of-the-Art Superpixel Methods," in *IEEE Transactions on Pattern Analysis and Machine Intelligence*, vol. 34, Nov. 2012, pp. 2274-2282.

Figure Legends

Figure 1: Usage examples of ε-filter and region of interest to focus on desirable skin features. From left to right, the first snapshot is the unprocessed permittivity map of volar forearm from a 64 years old male during arm extension. The second snapshot demonstrates how ε-filter removes the bad contact. The last image shows how we exclude the skin and sweat information with the ε-filter and the sensor borders with a circular region of interest while maintaining information on skin lines and furrows.

Figure 2: Example of micro-relief orientation analysis with anisotropy index calculation from permittivity image (a) without and (c) with ε-filter. The sample is captured from the volar forearm of a 64 years old volunteer with the arm at resting position. In (b) and (d), the highest correlation peak (135°) relates to Langer's lines and the lower correlation peak (45°) shows weaken elastic fibres network. The anisotropy index in (b) is 16.9 while in (d) is 38.6. This demonstrates the difference between studying the orientation of all components and focusing on specific value range.

Figure 3: Application of Vincent & Soille segmentation algorithm on permittivity image in palm area. Left the original image and right the segmented image with the borders of the skin closed polygons marked in blue. This demonstrates how a segmentation algorithm is capable to detect the skin polygons and mark the skin furrows around them. After detection, we can count the number of polygons and their surface area automatically.

Figure 4: Total skin lines correlation change during arm extension against chronological age.

Figure 5: Anisotropy index against chronological age.

Figure 6: Average number of closed polygons per mm² against chronological age.
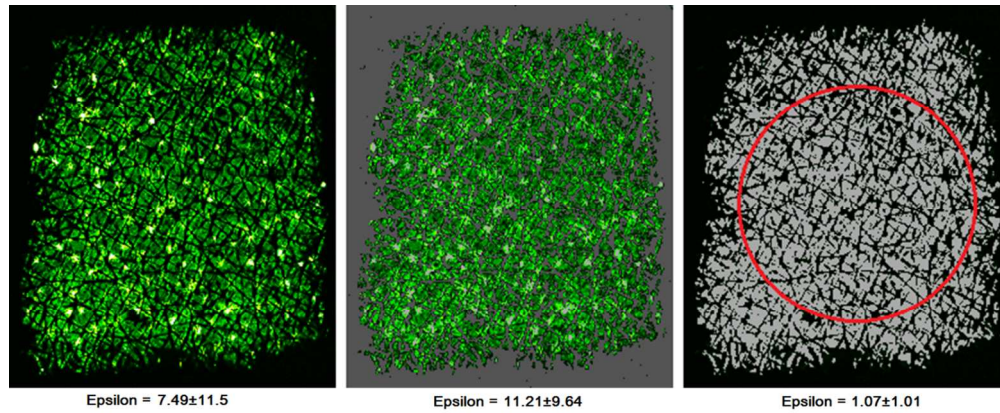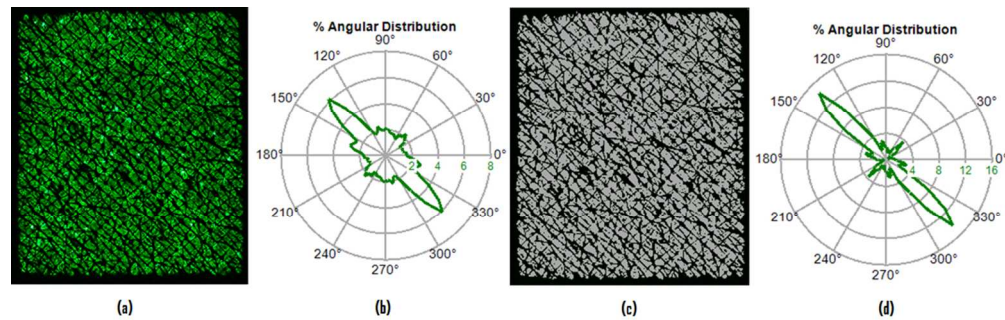
Table of Figures

Figure 1: Usage examples of ε-filter and region of interest to focus on desirable skin features. From left to right, the first snapshot is the unprocessed permittivity map of the volar forearm from a 64 years old male during arm extension. The second snapshot demonstrates how ε-filter removes the bad contact. The last image shows how we exclude the skin and sweat information with the ε-filter and the sensor borders with a circular region of interest while maintaining information on skin lines and furrows.

1
2
3
4
5
6
7
8
9
10
11
12
13
14
15
16
17
18
19
20
21
22
23
24
25
26
27
28
29
30
31
32
33
34
35
36
37
38
39
40
41
42
43
44
45
46
47
48
49
50
51
52
53
54
55
56
57
58
59
60

Figure 2: Example of micro-relief orientation analysis with anisotropy index calculation from permittivity image (a) without and (c) with ε-filter. The sample is captured from the volar forearm of a 64 years old volunteer with the arm at resting position. In (b) and (d), the highest correlation peak (135°) relates to Langer's lines and the lower correlation peak (45°) shows weaken elastic fibres network. The anisotropy index in (b) is 16.9 while in (d) is 38.6. This demonstrates the difference between studying the orientation of all components and focusing on specific value range.
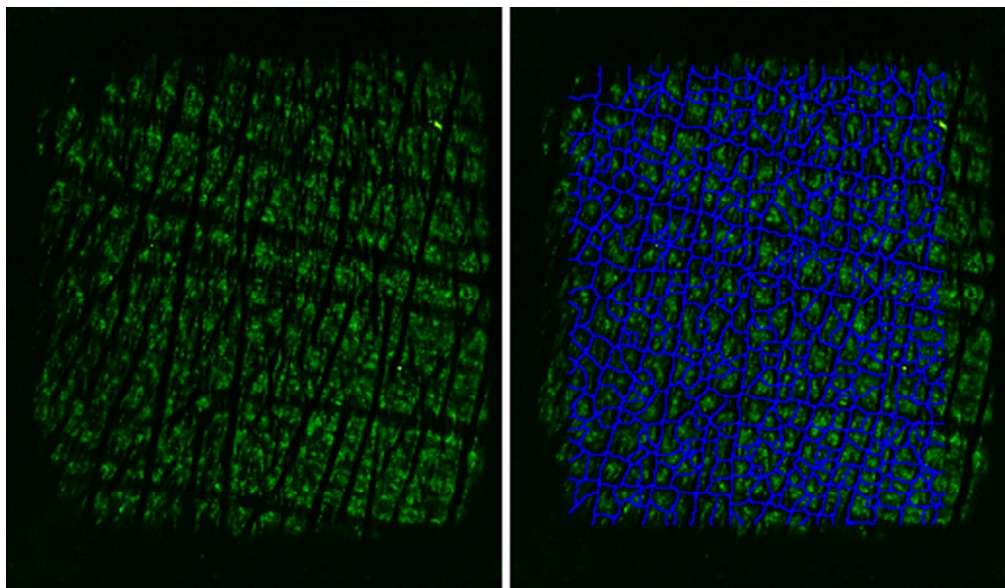
Figure 3: Application of Vincent & Soille segmentation algorithm on permittivity image in the palm area. Left the original image and right the segmented image with the borders of the skin closed polygons marked in blue. This demonstrates how a segmentation algorithm is capable to detect the skin polygons and mark the skin furrows around them. After detection, we can count the number of polygons and their surface area automatically.
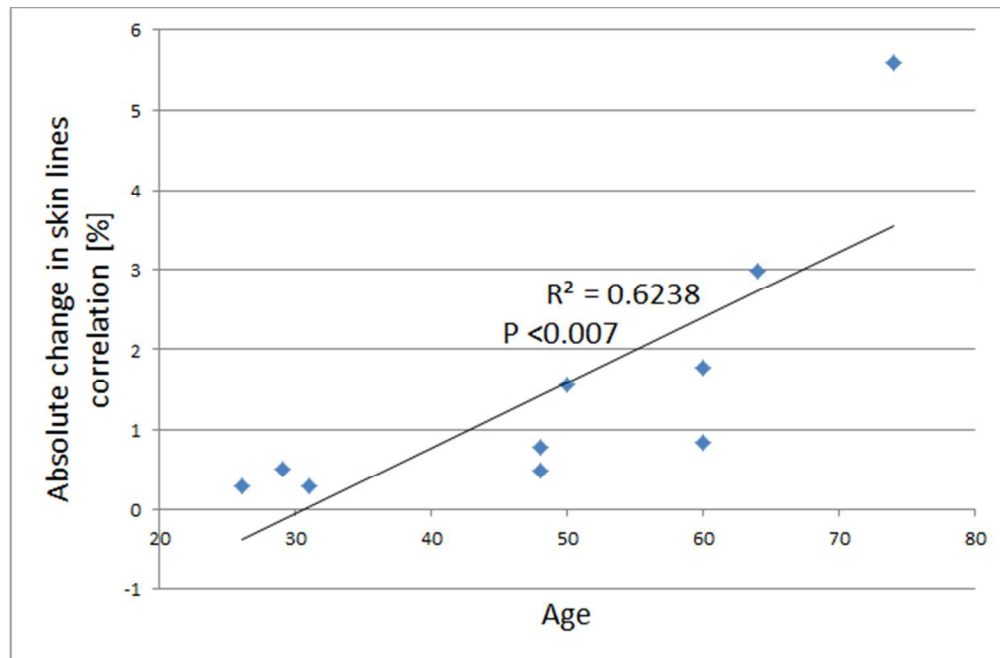
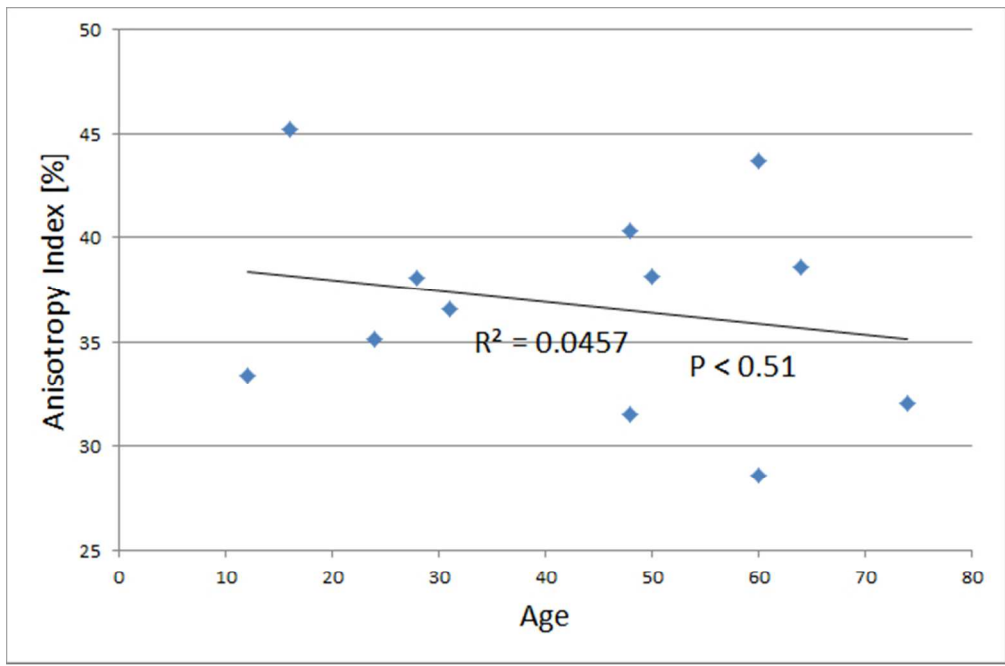Figure 4: Total skin lines correlation change during arm extension against chronological age.

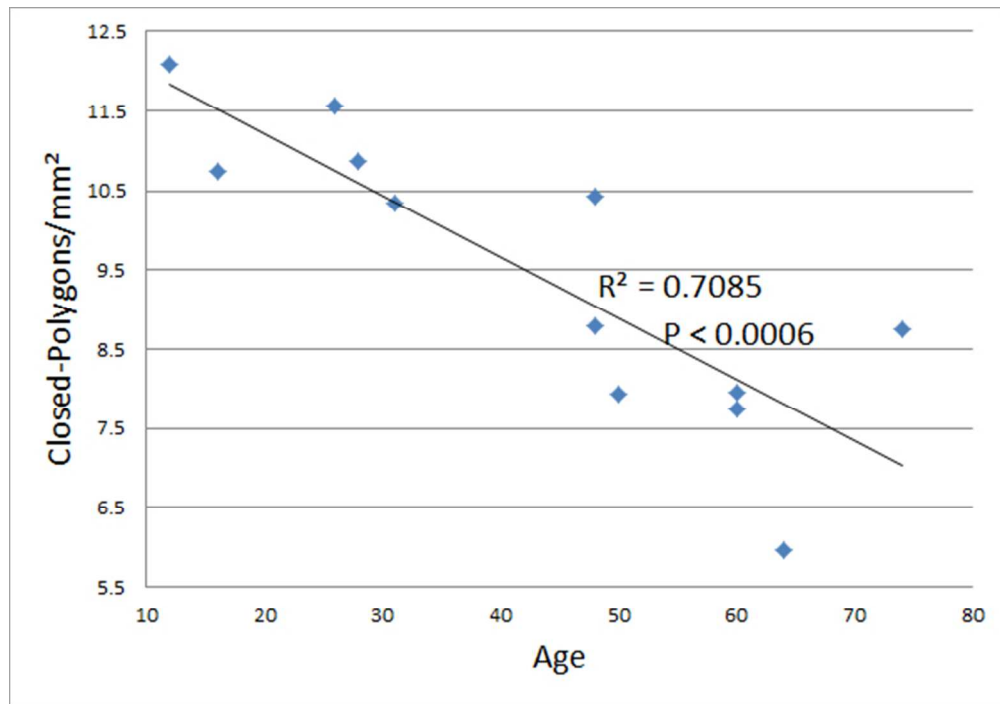Figure 5: Anisotropy index against chronological age.

Figure 6: Average number of closed polygons per mm² against chronological age.